JOURNAL OF MATERIALS SCIENCE 7 (1972) 813–821

Flux growth of some complex oxide materials

BARBARA M. WANKLYN
Clarendon Laboratory, University of Oxford, UK

This paper describes the preparation of the following complex oxide crystals which have not previously been grown by the flux method: $FeNbO_4$, $MnWO_4$, $CoWO_4$, $NiWO_4$, RMn_2O_5 (R = Er to Sm, and Y), $RMnO_3$ (R = Er to Gd), LaOCl, $La_2Ti_2O_7$, $Bi_2Sn_2O_7$, and $PbTiP_2O_8$. Single crystal X-ray diffraction data are reported for the latter material, the preparation of which has not previously been reported, and for $La_2Ti_2O_7$ and $Bi_2Sn_2O_7$, for which only powder data were previously available. Improved methods for the growth of Mn_3O_4, $LaCoO_3$, RPO_4 (R = Yb to Gd), $RCrO_3$ (R = Lu, Yb), ErOF and $NaNbO_3$ are also reported.

1. Introduction

Crystals large enough for many physical experiments can be produced by the flux method, the advantages of which have been previously described [1]. The chief disadvantage of the flux method, that of the incorporation of ions from the flux in the crystal lattice, is not serious for many applications and measurements. The present paper describes the preparation of some complex oxide crystals; research in progress on these crystals includes studies of magnetic transitions, magneto-electric behaviour, Mossbauer spectra, electrical conductivity, neutron diffraction and optical properties.

2. Experimental

The starting materials were of BDH laboratory reagent grade, with the following exceptions: the rare earth oxides were 99.9% pure, the PbO and Al_2O_3 were of "Analar" grade, and the PbF_2 was "extra pure". Pure platinum crucibles of 50 and 100 ml capacity, with closely fitting lids, were used. The apparatus and procedure have been described previously [2]. Hot-pouring techniques were used to separate crystals from molten flux [3, 4].

Tables I to IV give details of the compositions and experimental conditions. All the crystal products have been identified by the X-ray powder method. The major observations relating to each table were as follows:

2.1. Niobates and tungstates

Some of the transition metal tungstates have been pulled from the melt [5], but the growth of $FeNbO_4$ has not previously been reported.

Attempts to prepare transition metal niobates from Bi_2O_3 or PbO-PbF_2 solvents were unsuccessful, as the solutes combined with the flux and pyrochlore type structures were formed. Sodium ditungstate, which has previously been used for the flux growth of materials such as ferrites [6] and alkaline earth tungstates [7],

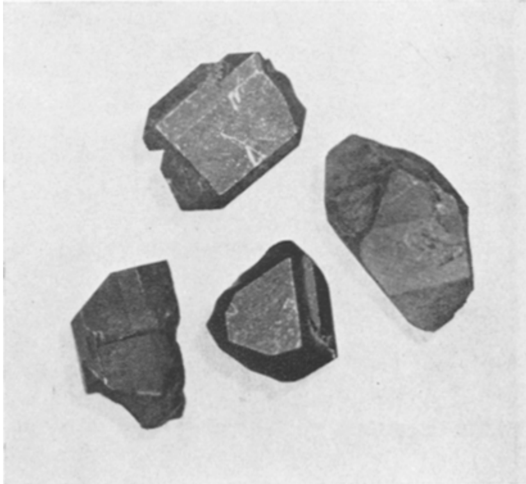
Figure 1 $CoWO_4$ (× 4).

TABLE I Compositions and flux growth conditions for niobates and tungstates.

Compound	Starting composition	Crucible volume (ml)	Initial temp. (°C)	Holding time (h)	Final temp. (°C)	Cooling rate (°C/h)	Product
$FeNbO_4$	9.6 g Fe_2O_3, 16 g Nb_2O_5, 94.4 g Na_2WO_4, 18.4 g WO_3	100	1250	15	600	1.5	Black octahedra (2 × 2 × 3) mm^3
$MnWO_4$	6 g $MnCO_3$, 48 g Na_2WO_4, 9.5 g WO_3	50	1250	15	600	1.5	(3 × 3 × 3) mm^3 dark purple crystals
$CoWO_4$	7.5 g CoO, 53.4 g Na_2WO_4, 10.5 g WO_3	50	1250	15	600	1.5	(4 × 4 × 4) mm^3 dark blue crystals
$NiWO_4$	3 g NiO, 53.4 g Na_2WO_4, 10g WO_3	50	1250	15	600	1.5	(6 × 6 × 6) mm^3 brownish crystals
$NaNbO_3$	16 g Nb_2O_5, 107 g Na_2WO_4, 21 g WO_3	100	1260	2	950	2	Colourless pseudocubes (6 × 6 × 3) mm^3

TABLE II Compositions and flux growth conditions for manganites.

Compound	Starting composition	Crucible volume (ml)	Initial temp. (°C)	Holding time (h)	Final temp. (°C)	Cooling rate (°C/h)	Product
RMn_2O_5 (R = Er to Sm, and Y)	9.2 g R_2O_3, 11.5 g $MnCO_3$, 1 g B_2O_3, 36 g PbO, 54 g PbF_2, 3.3 g PbO_2	50	1280	15	950	1.2	Shiny black prisms up to (7 × 5 × 5) mm^3
Mn_3O_4	26 g $MnCO_3$, 2 g B_2O_3, 72 g PbO, 103 g PbF_2, 6.6 g PbO_2	100	1280	15	950	1.2	Black octahedral crystals, (111) facets up to (10 × 10) mm^2
$GdMnO_3$ (orthorhombic)	18 g Gd_2O_3, 11.4 g $MnCO_3$, 58 g PbF_2	50	1290	—	1180	1	Black pseudocubes (3 × 3 × 2) mm^3
$ErMnO_3$ (hexagonal)	6.7 g Er_2O_3, 7.7 g $MnCO_3$, 1 g B_2O_3, 7 g PbO, 56 g PbF_2, 3.3 g PbO_2	50	1280	15	900	1	Thin black basal plates ~ 20 mm^2

proved very suitable for the transition metal tungstates (fig. 1), for $FeNbO_4$ (fig. 2) and for $NaNbO_3$. Evaporation of the flux was negligible at 1260° C and the crucibles were not attacked.

Analysis of the $FeNbO_4$ crystals yielded the composition: 26% Fe, 45% Nb, and 0.6% W, in good agreement with the calculated composition, 26% Fe, 44% Nb. EPMA showed that the crystals contained microscopic inclusions of α-Fe_2O_3.

2.2. Manganites

$RMnO_3$. The hexagonal manganites $RMnO_3$ (R = Ho to Lu) have previously been grown from Bi_2O_3 [8] and from PbO-Bi_2O_3 [9] solvents. These fluxes have the disadvantage that they attack platinum crucibles severely, and since Bi^{3+} is similar in size and charge to R^{3+}, it tends to replace R^{3+} in the crystal lattice. For example, $GdAlO_3$ crystals grown from Bi_2O_3/B_2O_3 flux

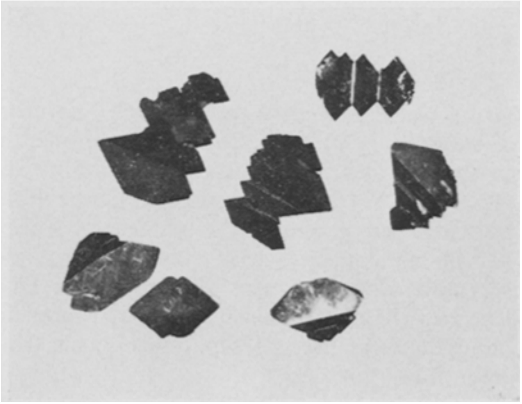

Figure 2 $FeNbO_4$ (× 3.2).

TABLE III Compositions and flux growth conditions for other rare earth compounds.

Compound	Starting composition	Crucible volume (ml)	Initial temp. (°C)	Holding time	Final temp. (°C)	Cooling rate (°C/h)	Product
$LaCoO_3$	1.6 g La_2O_3, 0.4 g CoO, 6 g PbF_2, 8 g PbO, 1.2 g PbO_2	10	1250	6 days			Black pseudocubes $(2 \times 1 \times 1)$ mm^3
$La_2Ti_2O_7$	9.8 g La_2O_3, 4.8 g TiO_2 54 g PbF_2, 49 g PbO, 3.0 g B_2O_3, 2 g PbO_2	50	1230	3 days			Thin yellowish platelets (4×5) mm^2
$HoPO_4$ (tetragonal)	5 g Ho_2O_3, 100 g $Pb_2P_2O_7$	50	1370		950	1	Clear tetragonal prisms $(20 \times 2 \times 2)$ mm^3
$GdPO_4$ (monoclinic)	6 g Gd_2O_3, 100 g $Pb_2P_2O_7$	50	1370		950	1	Prisms $(7 \times 1.5 \times 0.6)$ mm^3
LaOCl (1)	3 g $LaCl_3$	10	1050	2 h			(3×3) mm^2 platelets
(2)	4.5 g $MgSO_4$ + 6.9 g $LaCl_3$	10	1050	2 h			(3×3) mm^2 flat transparent platelets
ErOF	120 g Er_2O_3, 50 g Fe_2O_3, 356 g PbF_2, 237 g PbO, 12.5 g B_2O_3, 5.0 g PbO_2	500	1255	1 h	940	1	Clear pink plates up to 1 mm thick, (20×5) mm^2
$YbCrO_3$	11.2 g Yb_2O_3, 2.2 g Cr_2O_3, 75 g PbF_2, 4.2 g B_2O_3, 0.7 g PbO_2	50	1260	9 days			Shiny faceted crystals up to $(3 \times 3 \times 2)$ mm^3
$LuCrO_3$	10 g Lu_2O_3, 2.9 g Cr_2O_3, 75 g PbF_2, 1 g B_2O_3, 0.7 g PbO_2	50	1260	9 days			Well-formed crystals $(3 \times 2 \times 2)$ mm^3 + $LuBO_3$

TABLE IV Compositions and flux growth conditions for other oxide materials

Compound	Starting composition	Crucible volume (ml)	Initial temp. (°C)	Holding time	Final temp. (°C)	Cooling rate (°C/h)	Product
$PbTiP_2O_8$	4 g TiO_2, 70 g $Pb_2P_2O_7$	50 cc	1280	15 h	910	2	Twinned, colourless plates, up to (4×1.5) cm^2, 0.5 mm thick
$Bi_2Sn_2O_7$	(1) 14 g Bi_2O_3, 9 g SnO_2, 72 g PbF_2	50 cc	1280	16 h	900	6	Reddish crystals $(2 \times 2 \times 2)$ mm^3
	(2) 4.7 g Bi_2O_3, 2 g SnO_2, 30 g KF	100 cc	1100	1 h	850	6	Clear yellow octahedra $(1 \times 1 \times 1)$ mm^3

were found to contain 5.5% Bi [2]. Using the less corrosive flux PbO-PbF_2, $RMnO_3$ platelets have been grown at slow cooling rates, such as 2°/h. Removal of the flux while still liquid is particularly advantageous for the recovery of these thin, relatively large basal plates, shown in fig. 3.

Whereas the hexagonal manganites were relatively free from the phase RMn_2O_5, in the case of the orthorhombic perovskites $RMnO_3$ (R = La to Dy) there was an increasing tendency for RMn_2O_5 to form with decreasing ionic radius of R^{3+}. In some batches intended to yield $GdMnO_3$, $GdMn_2O_5$ was the sole product; in others, the crystals which grew at the base of the crucible consisted of $GdMnO_3$ only, but those which grew at the melt surface were covered with a layer of $GdMn_2O_5$. It appeared that the more highly oxidized phase RMn_2O_5 was favoured at lower temperatures (1100 to 900°C). Reproducible growth of $GdMnO_3$, $TbMnO_3$ and $DyMnO_3$ was finally achieved by slowly cooling a saturated solution of the components in PbF_2 from 1280 to 1180°C. At these temperatures, evaporation of the flux contributes to crystal growth; the best results were obtained when the flux had evaporated entirely, avoiding the subsequent need to clean the crystals in hot dilute

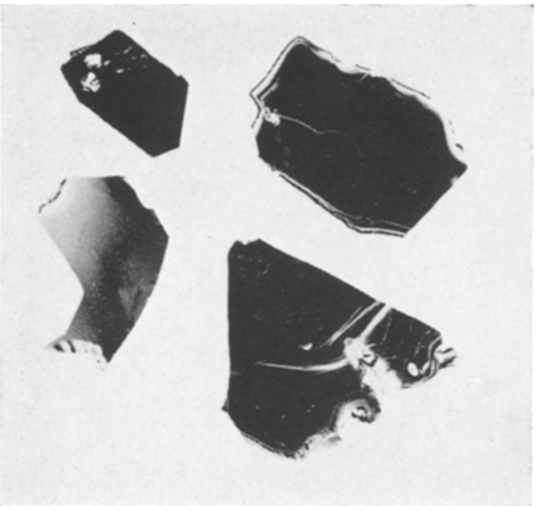

Figure 3 Platelets of $ErMnO_3$ (× 4).

acid, in which they partially dissolve. A starting composition corresponding to 43 g $GdMnO_3$ in 100 g PbF_2 was used, indicating remarkably high solubility of the $RMnO_3$ phase. $GdMnO_3$ crystals are semi-conducting; preliminary measurements show complex behaviour with resistivity of the order 10^2 ohm cm using a voltage between 1 and 10 V. This property was used to separate these crystals from $GdMn_2O_5$ (resistivity 10^{10} ohm cm), when both phases were present. $GdMnO_3$ crystals are shown in fig. 4.

RMn_2O_5. Crystals (R = Er to Sm, and Y) were grown from PbO-PbF_2-B_2O_3 flux. With the smaller rare earth ions which form the hexagonal phase $RMnO_3$, such as Er^{3+}, however, this phase was less stable with respect to Mn_3O_4 and $RMnO_3$. The RMn_2O_5 prisms were characteristically shiny and had narrow corner facets, as shown in fig. 5. Analysis carried out by Johnson Matthey Chemicals Ltd gave a lead content of 0.4%.

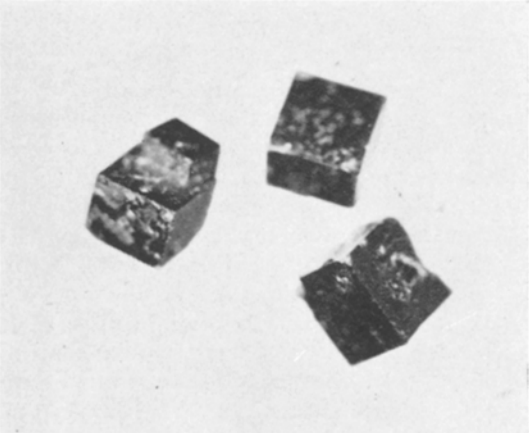

Figure 4 $GdMnO_3$ (× 7).

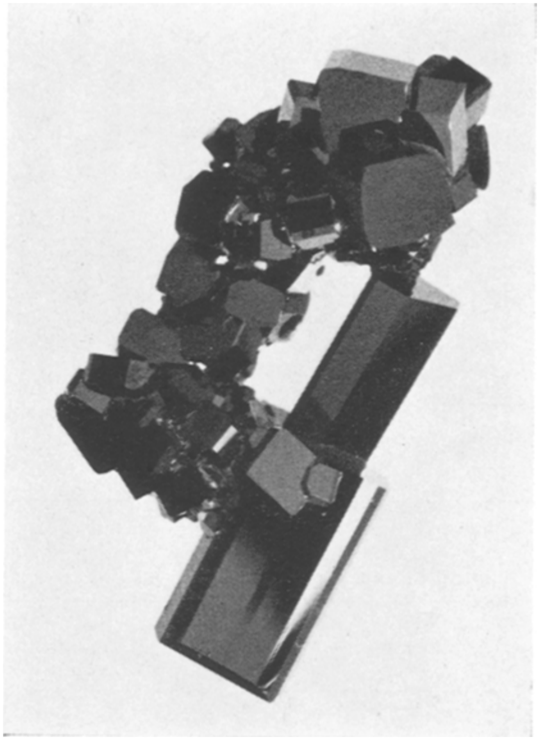

Figure 5 $TbMn_2O_5$ (× 3.5).

Mn_3O_4. This material grew as rods and octahedra, some with relatively perfect faces up to 1 cm on edge as shown in fig. 6. A dendritic internal structure was revealed when flux inclusions were dissolved in hot dilute HNO_3.

2.3. Other rare earth compounds

$LaCoO_3$. PbO has been used as flux for the perovskite $LaCoO_3$ [10], but this solvent attacks platinum crucibles so severely that slow cooling rates are not practical. The addition of PbF_2 enabled crystals to be obtained without damage to the crucibles. At high concentrations of PbF_2, however, LaF_3 is formed.

$La_2Ti_2O_7$. $La_2Ti_2O_7$ differs from the other $R_2Ti_2O_7$, pyrochlore, compounds in having a layer structure [11]. From PbO-PbF_2 solution, the material grew as needles only, but when 3% B_2O_3 was added to the flux large thin platelets

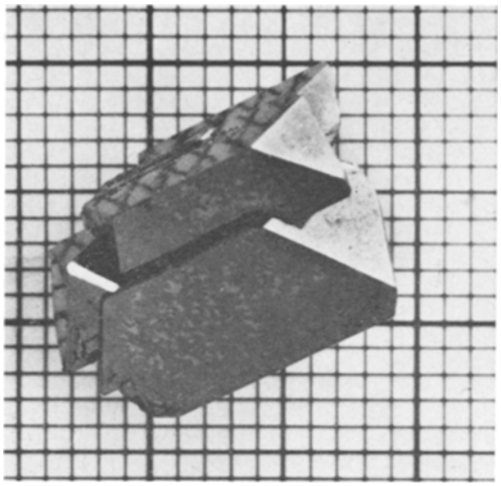

Figure 6 Mn_3O_4 (mm grid).

were formed, and these showed sharp extinction under the polarizing microscope. Preliminary work on the structure indicates an orthorhombic unit cell with dimensions 5.60, 7.85 and 51.5 Å, the last dimension being in the direction normal to the plate [12].

RPO_4. The flux $Pb_2P_2O_7$ [13] was found to be particularly suitable for the growth of RPO_4, and in these experiments BDH material was premelted to reduce its volume prior to the addition of the solute. Clear rods of the tetragonal RPO_4 compounds (R = Tm to Tb) up to (20 × 2 × 2) mm^3 and plates up to (20 × 4 × 0.5) mm^3 were obtained from 50 ml crucibles by slowly cooling from 1370°C. Fig. 7 shows platelets of $TmPO_4$. Repeated runs from this temperature did not damage the crucibles. With R = Gd, crystals with the monoclinic monazite structure were produced as transparent prisms up to (7 × 1.5 × 0.5) mm^3, as shown in fig. 8.

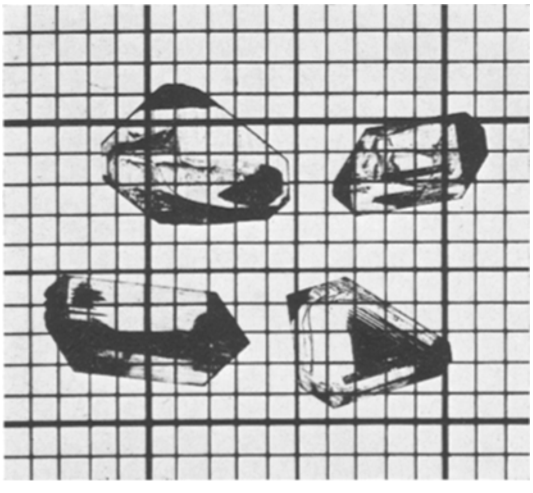

Figure 7 Tetragonal phosphate $TmPO_4$ (mm grid).

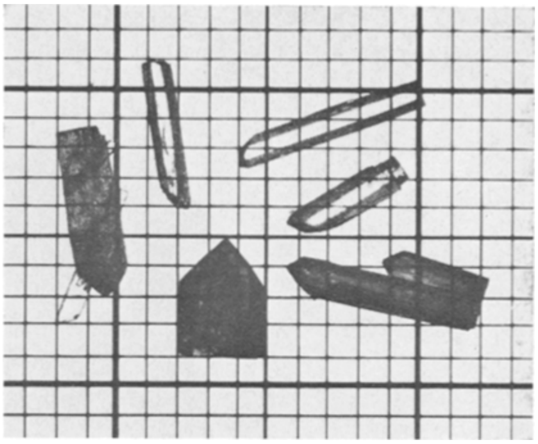

Figure 8 Monoclinic phosphate $GdPO_4$ (mm grid).

ROCl. LaOCl is an effective host lattice for rare-earth activators which fluoresce in the visible region of the spectrum [14]. Material prepared previously by heating the chlorides at 100 to 500°C, or by reacting R_2O_3 with excess NH_4Cl at 800 to 1000°C [14], was reported to yield particles only a few microns in size.

By rapidly heating anhydrous $LaCl_3$ in a closed crucible to 1050°C and holding at this temperature for 2 h, thin curved platelets of LaOCl several mm across were grown. $ErCl_3$ similarly treated yielded needles of ErOCl. Growing the compounds in an open crucible, or using hydrated RCl_3 as raw material in a closed crucible, yielded only a powdery material. The oxychloride crystals are apparently produced as a result of the sequence of two processes: hydrolysis of the chloride melt, followed by evaporation of the chloride. The process is analogous to that described by Dugger [15] for the growth of oxide crystals by hydrolysis of fluoride solutions. Addition of 65 wt % of dehydrated $MgSO_4$ to the $LaCl_3$ resulted in better formed, rectangular, flat crystal plates. The platelets, shown in fig. 9, were transparent and optically isotropic, indicating that the tetragonal *c*-axis was perpendicular to the plane of the platelets.

ErOF. As reported previously [1], 1 to 2 mm crystals of ROF may be grown from PbO/PbF_2 mixtures containing both R_2O_3 and Al_2O_3. Much larger crystal plates can be grown, how-

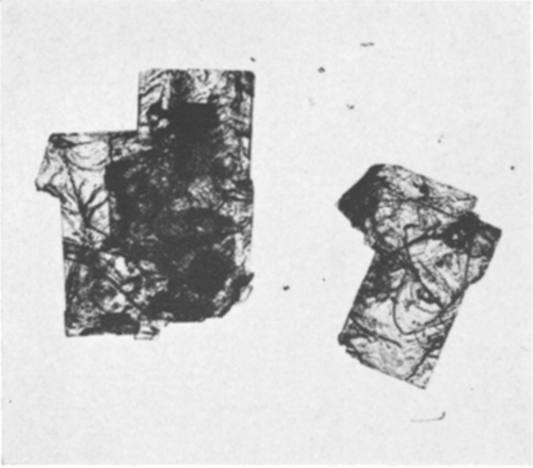

Figure 9 LaOCl platelets (× 13.3).

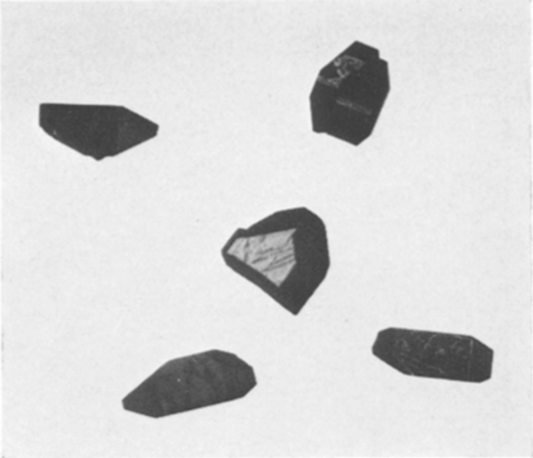

Figure 11 $YbCrO_3$ (× 4).

ever, if Al_2O_3 is replaced by Fe_2O_3 and the system is sealed, maintaining the F^- concentration at a constant level, as both preferential evaporation of PbF_2 and hydrolysis of the melt are prevented thereby. In practice, a lid was welded to the crucible and a small hole made in the lid so that the pressure on the crucible remained atmospheric during the experiment. Transparent crystal plates up to 2 cm on edge were obtained. Fig. 10 shows ErOF crystals with erbium iron garnets, embedded in flux as they grew adjacent to the crucible wall.

$RCrO_3$ (R = Lu, Yb). A previous publication [1] described the growth of rare earth orthochromites by evaporation of $PbO/PbF_2/B_2O_3$ flux using stoichiometric weights of R_2O_3 and Cr_2O_3. With the smaller rare earth ions, this method produced ill-formed crystal sheets without characteristic facets.

It has been found that addition of excess

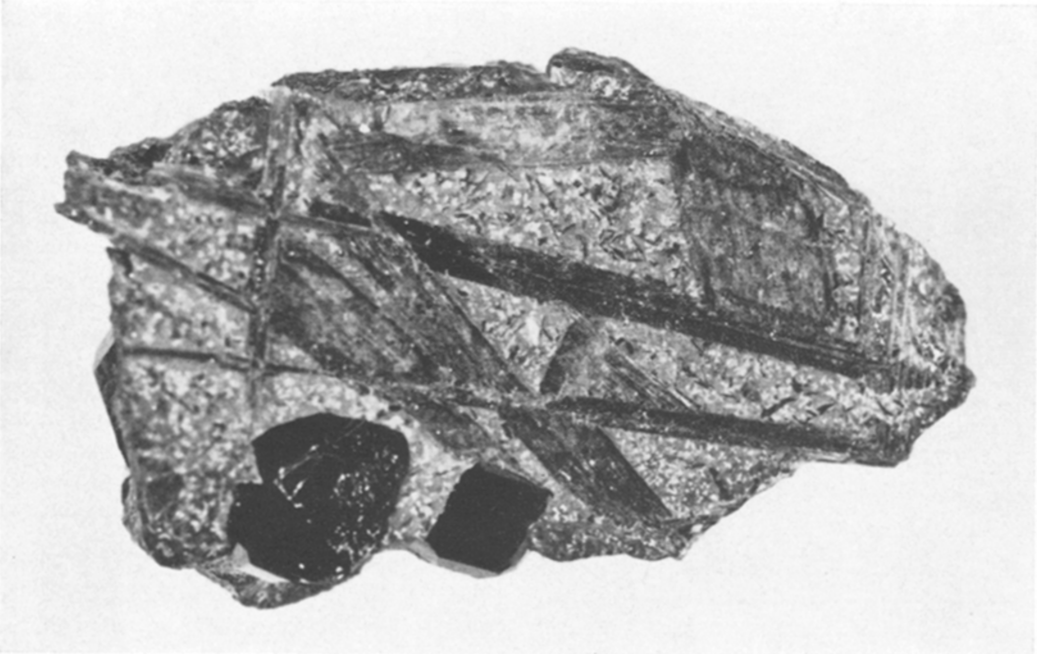

Figure 10 ErOF platelets and erbium iron garnets in flux (× 5).

R_2O_3 (R_2O_3:Cr_2O_3 approx. 2:1) greatly improved the quality of the crystals. With $YbCrO_3$, a layer of YbOF formed at the melt surface, restricting the rate of evaporation, and shiny well-faceted pseudocubes shown in fig. 11 grew below. With $LuCrO_3$ (fig. 12), $LuBO_3$ also formed, and it was necessary to reduce the B_2O_3 content in the mixture to prevent this.

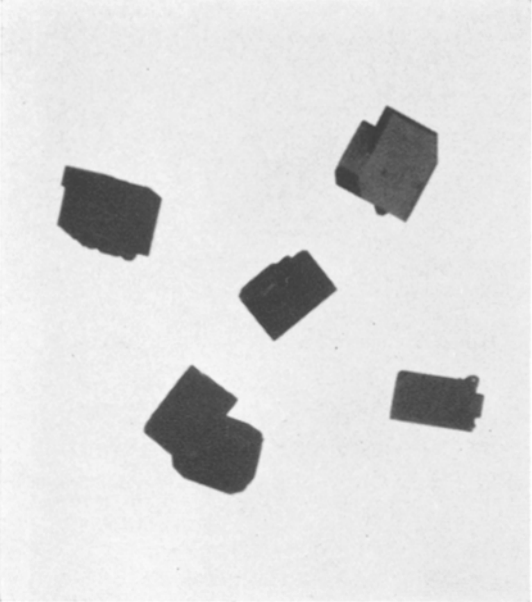

Figure 12 $LuCrO_3$ (× 5).

2.4. Other oxide materials

$PbTiP_2O_8$. This previously unreported material was obtained in the form of large twinned crystal plates (fig. 13) by slowly cooling a solution of TiO_2 in $Pb_2P_2O_7$. Observation with a polarizing microscope revealed the twin structure which is shown in fig. 14. Material which gave the same X-ray powder pattern as the crystal plates was produced by fusing a stoichiometric mixture of PbO, TiO_2 and $2NH_4H_2PO_4$. The weight loss during reaction of these materials was only 3% in excess of theoretical. A rapidly melted portion of the product on examination with a polarizing

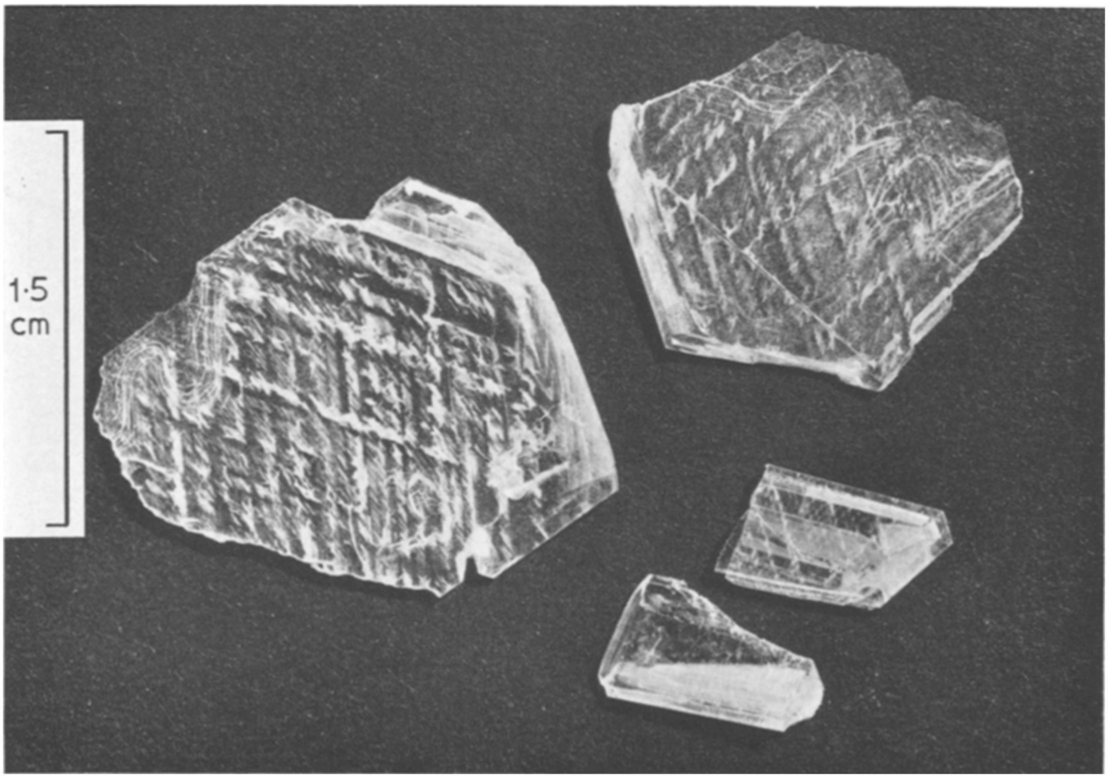

Figure 13 $PbTiP_2O_8$ platelets (× 3.5).

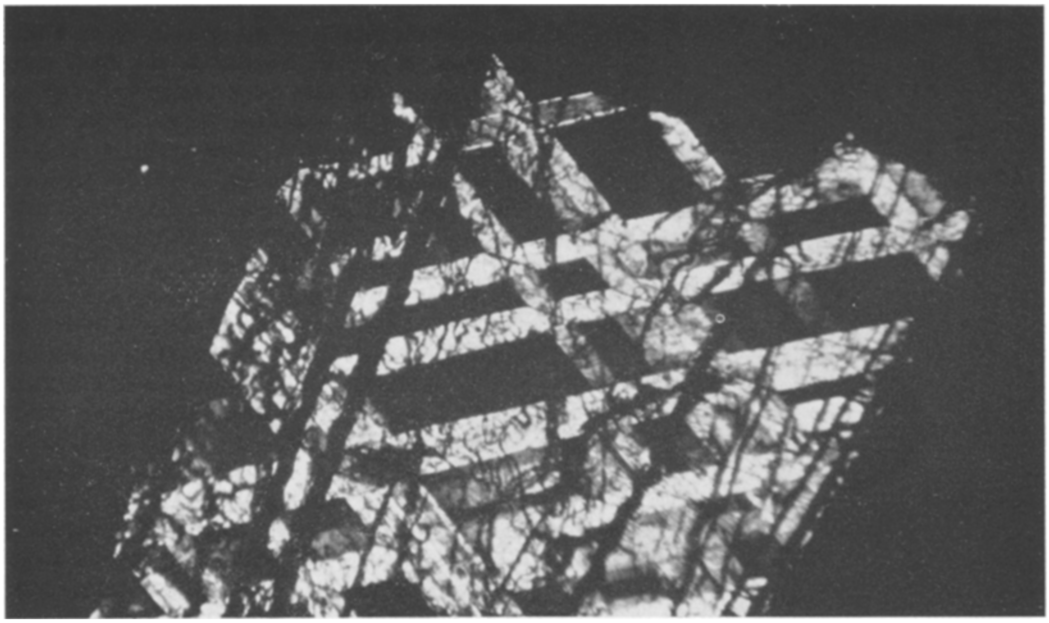

Figure 14 Twin structure in $PbTiP_2O_8$ (× 25).

microscope showed no sign of glassy fragments; all the material was optically anisotropic.

Observation with a hot stage microscope of a crystal plate showed a reversible phase transition at 1140°C (private communication, E. A. D. White). Holding at this temperature for a few minutes resulted in loss of PbO and formation of glassy material.

We can conclude that the composition $PbTiP_2O_8$ corresponds to that of the crystal plates. The diffraction pattern can be indexed to a monoclinic lattice for which the lattice parameters are $a_0 = 8.14$ Å, $b_0 = 5.12$ Å, $c_0 = 14.9$ Å, $\beta = 93.2°$ [16].

$Bi_2Sn_2O_7$. This material has a structure which differs from the normal pyrochlore. Single crystal X-ray photographs using crystals grown from KF solution indicate a face-centred cubic unit cell for which $a_0 = 21.360 \pm 0.001$ Å [11], in agreement with the value suggested by Roth [10] from a study of sintered samples of $Bi_2Sn_2O_7$.

3. Conclusion

The methods described above have proved to be suitable for the reproducible preparation of complex oxide crystals. Although the batch quantities are small, the size and quality of the crystals are adequate for many studies of their properties.

Acknowledgements

The author thanks Dr G. Garton and Dr S. H. Smith of this laboratory, and Dr E. A. D. White of Imperial College, London, for helpful discussions, Dr M. Poole of AERE, Harwell, for the analysis of $FeNbO_4$, G. Gwynn and P. Clack for technical assistance, and the photographic section of this department for the plates.

This work was supported in part by the Science Research Council.

References

1. G. GARTON and B. M. WANKLYN, *J. Mater. Sci.* **3** (1968) 395.
2. B. M. WANKLYN, *J. Crystal Growth* **5** (1969) 323.
3. G. GARTON and B. M. WANKLYN, Paris-Grenoble Colloque International sur les Elements des Terres Rare (1969), Tome 1, 343.
4. G. GARTON, S. H. SMITH, and B. M. WANKLYN, *ICCG* 3 (in press).
5. L. G. VAN UITERT, J. J. RUBIN, and W. A. BONNER, *J. Amer. Ceram. Soc.* **46** (1963) 512.
6. W. KUNNMANN, A. FERRETTI, R. J. ARNOTT, and D. B. ROGERS, *J. Phys. Chem. Solids* **26** (1965) 311.
7. L. G. VAN UITERT, *J. Phys. Chem. Solids* **25** (1964) 1447.

8. E. F. BERTAUT and F. FORRAT, British Patent 979 (1965) 546.
9. H. TAMURA, E. SAWAGUCHI, and A. KIKUCHI, *Japan J. Appl. Phys.* **4** (1965) 621.
10. J. P. REMEIKA, *J. Amer. Chem. Soc.* **78** (1956) 4259.
11. R. S. ROTH, *J. Res. Nat. Bur. Stad.* **56** (1956) 17.
12. V. SEIDL and O. KNOP, Dalhousie University, Halifax, Nova Scotia, private communication.
13. R. FEIGELSON, *J. Amer. Ceram. Soc.* **47** (1964) 257.
14. S. NATANSOHN, Paris-Grenoble Colloque International sur les Elements des Terres Rares (1969), Tome 1.
15. C. O. DUGGER, *Proc. ICCG Boston, USA*, ed. H. S. Peiser, Pergamon Press (1966) 493.
16. J. G. SCANE, Portsmouth Polytechnic, private communication.

Received 25 November and accepted 30 December 1971.